Spin-conserving and spin-flipping equation-of-motion coupled-cluster method with triple excitations

Lyudmila V. Slipchenko and Anna I. Krylov[a)]
Department of Chemistry, University of Southern California, Los Angeles, California 90089-0482

(Received 15 June 2005; accepted 29 June 2005; published online 30 August 2005)

We report the implementation of the spin-conserving and spin-flipping variants of the equation-of-motion (EOM) coupled-cluster (CC) model, which includes single and double excitations in the CC part and single, double, and triple excitations in the EOM part, i.e., EOM-CC(2,3) [Hirata, Nooijen, Bartlett, Chem. Phys. Lett. **326**, 255 (2000)] for closed- and open-shell references. Inclusion of triples significantly improves the accuracy of EOM-CCSD for excitation energies (EOM-EE-CCSD) and its spin-flip (SF) counterpart, EOM-SF-CCSD, especially when the reference wave function is strongly spin-contaminated. A less computationally demanding active space variant with semi-internal triples has also been implemented. The capabilities of full and active space EOM-CC(2,3) are demonstrated by applications to CO^+ and CH radicals as well as to the methylene and trimethylenemethane diradicals and the dehydro-*m*-xylylene triradical. © *2005 American Institute of Physics*. [DOI: 10.1063/1.2006091]

I. INTRODUCTION

Equation-of-motion coupled-cluster (EOM-CC) method and closely related linear response theory (LRT) are two powerful tools for accurate and robust calculations of electronically excited and open-shell species. EOM-CC with single and double excitations (EOM-CCSD)[1–3] describes electronic states with predominantly singly excited character with accuracy of 0.1–0.2 eV.[4] Unfortunately, the EOM-CCSD performance deteriorates for electronic states with large contributions of double excitations as, for example, dark states of polyenes or some valence states of radicals. Moreover, the EOM-CCSD accuracy degrades when the reference wave function is spin-contaminated. The inclusion of triple excitations rectifies these problems, which originate in incomplete treatment of nondynamical correlation, and also improves accuracy for well-behaved excited states by more complete accounting of dynamical correlation. For example, the error bars of EOM-CCSDT are 0.1 eV for the states with large doubly excited character and 0.01 eV for singly excited states.[4,5]

An overview of the high-level CC and EOM-CC models can be found, e.g., in Ref. 6. Similar ideas were explored within the so-called general-*R* symmetry-adapted-cluster configuration-interaction (SAC-CI) formalism.[7,8] Several approaches that incorporate triple excitations in EOM-CC were reported.[9–21] Implementations of full EOM-CCSDT, EOM-CCSDTQ, and even EOM-CCSDTQP were reported,[15,17–19] as well as a variety of approximations of the full EOM-CCSDT. For example, Watts and Bartlett implemented an approximate EOM-CCSDT model, in which only two-body elements in the triples block of the similarity-transformed Hamiltonian were included,[9] iterative EOM-CCSDT-1 and EOM-CCSDT-3 models and their non-iterative counterparts EOM-CCSD(T) and EOM-CCSD($\tilde{T}$).[10,11] The iterative CC3 and the non-iterative CCSDR(3) models were introduced by Koch and co-workers.[12–14]

Active space CC and EOM models were developed by Kowalski and Piecuch,[16,17] and by Krylov *et al.*[22] The initial benchmarks for these models included singlet and triplet excited states of closed-shell molecules, e.g., CH^+, C_2, N_2, and focused on accurate description of the excited states with a dominant doubly excited character, such as the $2\ ^1A_1$ state in methylene.

Another problem that benefits from inclusion of triples in EOM-CC is the excited states of radicals, especially when the reference state and, consequently, the excited state wave functions are strongly spin-contaminated. To this end, several methods were developed.[20,21] Szalay and Gauss introduced spin-restricted (SR) version of LRT with inclusion of the so-called pseudotriple (psT) excitations (SR-CCSD-LRT and CCSD-psT-LRT) and benchmarked it on the series of small radicals, i.e., OH, CN, CO^+, and CH.[20] Smith *et al.* implemented the open-shell variant of the CC3 method and applied it to low-lying electronic states of allyl and nitromethyl radicals.[21]

The spin-flip (SF) variant of EOM-CCSD, which employs a high-spin (triplet or quartet) Hartree-Fock determinant as a reference,[23,24] is also sensitive to spin-contamination of the reference. For example, in σ-π diradicals, the high-spin unrestricted Hartree-Fock (UHF) determinant may be spin-contaminated, which results in severe spin-contamination of the EOM target states.[25] The inclusion of triples, or a subset thereof, would reduce spin-contamination and improve accuracy in this case as well.

The inclusion of triple excitations for the excited states usually results in the computational scaling of N^7-N^8, where N is the size of the system, and is therefore computationally demanding. Consequently, a model with explicit full iterative triple excitations can be applied only to small molecules in a

[a)]Electronic mail: krylov@usc.edu

moderate basis set. However, several approaches exist to extend the scope of applicability of models with triple excitations to larger systems. These are energy separability schemes,[26] basis set extrapolations,[27–29] and those including only internal or semi-internal triple excitations.[16,17,20,22] These strategies allow one to evaluate the effects of triple and even quadrupole excitations in much larger systems.

In this work, we report the implementation and benchmarks of the EOM-CC(2,3) method, i.e., the EOM-CC model with inclusion of triples in the EOM part only. Both excitation energies (EE) and spin-flip variants of the method are implemented.

As shown by Hirata *et al.*,[5] the accuracy of EOM-CC(2,3) closely follows that of full EOM-CCSDT for singly and doubly excited states of closed-shell molecules. Our benchmarks demonstrate that this method performs very well for open-shell systems as well. As a less computationally demanding alternative, the active space EOM-CC(2,3) model [EOM-CC $(2,\tilde{3})$], in which only semi-internal triples are included, is also implemented. We benchmarked full and active space EOM-CC(2,3) on a number of radicals, diradicals, and triradicals.

A desired property of a correlated model is its insensitivity to the reference determinant. For example, the full configuration interaction method (FCI) is invariant with respect to the reference/orbitals choice; CCSD is less sensitive than lower level second order perturbation theory (MP2); etc. Overall, CCSD is rather insensitive to the reference choice; e.g., UHF- and restricted open-shell Hartree-Fock (ROHF) based CCSD or CCSD(T) results are usually similar.[30] However, this is less so for the EOM-CCSD target states. For example, when the reference UHF determinant is spin-contaminated, the EOM-CCSD states are very likely to be spin-contaminated, even though the CC ansatz almost completely restores the spin symmetry of the reference wave function. As a result, the UHF- and ROHF-based EOM excitation energies can differ by several tenths of eV. This unsatisfactory behavior was observed in the EOM-EE-CCSD calculations of radicals[20] and also in the EOM-SF-CCSD studies of σ-π diradicals and triradicals.[25]

As shown below, EOM-CC(2,3) is much less sensitive to the choice of a reference determinant than is EOM-CCSD. For example, the EOM-CC(2,3) excitation energies of CH differ only by thousandths of eV, whereas the corresponding differences between the UHF- and ROHF-based EOM-EE-CCSD energies are up to 0.4 eV.

Section II discusses the theoretical approach of full and active space EOM-CC(2,3); additional details are given in the Appendix. The results are presented in Sec. III. Our concluding remarks are given in Sec. IV.

II. THEORY AND COMPUTATIONAL DETAILS

A. EOM-CC(2,3)

In the EOM approach, the energies of target states E_k are found by diagonalizing the so-called similarity transformed Hamiltonian $\bar{H}=e^{-T}He^{T}$:

$$\bar{H}R(k) = E_k R(k), \tag{1}$$

where T and $R(k)$ are general excitation operators with respect to the reference determinant $|\Phi_0\rangle$.

The reference determinant $|\Phi_0\rangle$ defines a separation of the orbital space into a subspace of orbitals occupied in $|\Phi_0\rangle$ and a complementary subspace of virtual orbitals. We will adhere to the convention when indices $i,j,k,\ldots$are reserved for the orbitals occupied in the reference determinant $|\Phi_0\rangle$; indices $a,b,c,...$— for the unoccupied orbitals, and $p,q,r,s,\ldots$ are used in a general case, i.e., when an orbital can be either occupied or virtual. Then excitation and deexcitation operators can be represented as:

$$\begin{aligned} R &= R_0 + R_1 + \cdots + R_n, \\ L &= L_0 + L_1 + \cdots + L_n, \end{aligned} \tag{2}$$

where n is the highest excitation level, $R_0=r_0\hat{1}$, and the forms of R_k and L_k (as well as a definition of the excitation level k) depend upon the nature of the reference and final states. For example, when both the reference and the final states are states of the N-electron system, operators R_k and L_k conserve the number of electrons:

$$\begin{aligned} R_1^{\mathrm{EE}} &= \sum_{ia} r_i^a a^+ i, \\ L_1^{\mathrm{EE}} &= \sum_{ia} l_i^a i^+ a. \end{aligned} \tag{3}$$

When the reference and the final states differ by number of electrons, operators R_k/L_k^+ are ionizing (IP) or electron attaching (EA):

$$R_1^{\mathrm{IP}} = \sum_i r_i i, \tag{4}$$

$$R_1^{\mathrm{EA}} = \sum_a r_a a^+ \quad \cdots \tag{5}$$

$$R_1^{\mathrm{DIP}} = \sum_{ij} r_{ij} ji, \tag{6}$$

$$R_1^{\mathrm{DEA}} = \sum_{ab} r_{ab} a^+ b^+ \quad \cdots \tag{7}$$

Regardless of the choice of T, the spectrum of $\bar{H}$ is exactly the same as that of the original Hamiltonian H— thus, in the limit of the complete many-electron basis set, EOM is identical to FCI. However, in the case of truncated expansion, EOM is superior to CI in virtue of correlation effects being folded in through the similarity transformation. The convenient choice of amplitudes T, which offers several formal and numerical advantages, is from the CC equations for the reference state $|\Phi_0\rangle$:

$$\langle \Phi_\mu | \bar{H} - E | \Phi_0 \rangle = 0, \tag{8}$$

where Φ_μ denotes μ-tuple excited determinants, e.g., $\{\Phi_i^a, \Phi_{ij}^{ab}\}$ in the case of CCSD.

By combining different types of excitation operators and references $|\Phi_0\rangle$, different groups of target states can be accessed. For example, electronically excited states can be described when the reference $|\Phi_0\rangle$ corresponds to the ground state wave function, and operators $R(k)$ conserve the number of electrons and a total spin [see Eq. (3)], as in EOM-EE-CC.[1–3] In the ionized/attached EOM models, e.g., EOM-IP-CC and EOM-EA-CC, operators R [see Eqs. (4)–(7)] do not conserve total number of electrons.[31–33] These models can accurately treat ground and excited states of doublet radicals. In the EOM-SF-CC method, the excitation operators $R(k)$ include spin-flip of one electron.[23,24] This method accurately describes diradicals, triradicals, and bond-breaking.

Whereas the cluster operator T describes correlation in the reference wave function, the excitation operator $R(k)$ treats differential correlation effects between the reference and the target state wave functions. In practical applications, both T and $R(k)$ operators are truncated at some order, and therefore an approximate EOM-CC method is characterized by two parameters, m and n, i.e., the orders of T and $R(k)$, respectively, with each model being denoted by EOM-CC (m,n).[5]

In principle, T and $R(k)$ operators can be truncated at different levels. As demonstrated in Ref. 5 truncation of T and $R(k)$ at the same order (e.g., $m=n=2$, as in EOM-CCSD, or $m=n=3$, as in full EOM-CCSDT) results in the most balanced description of the excited states. However, the leading effect in capturing the accuracy of the description of the excited states is in the EOM rather than in the CC part:

$$\begin{aligned} &\mathrm{EOM-CC}(2,2)[\equiv \mathrm{EOM-CCSD}] \\ &\quad \simeq \mathrm{EOM-CC}(3,2) \ll \mathrm{EOM-CC}(2,3) \\ &\quad \simeq \mathrm{EOM-CC}(3,3)[\equiv \mathrm{EOM-CCSDT}], \end{aligned}$$

i.e., the accuracy of the EOM-CC(2,3) method closely follows that of full EOM-CCSDT [or EOM-CC(3,3)], whereas the computational cost of the former is less.

In the related SAC-CI method[7,8] the effective Hamiltonian does not have the same spectrum as the exact one, as the exponential part of the similarity transformation is truncated. Moreover, the SAC-CI triple and quadruple excitation operators are truncated to include only those with large weights, as estimated from the products of single and double excitation operators. Thus, both exponential and linear spaces of SAC-CI are arbitrarily truncated with respect to the same order EOM-CC. It is unclear how the threshold-based truncation affects the size-extensivity of the method.

This work presents our implementation of the EE and SF variants of EOM-CC(2,3), i.e., the EOM-CC model with

$$T = T_1 + T_2, \quad R(k) = R_0(k) + R_1(k) + R_2(k) + R_3(k), \tag{9}$$

as a less computationally demanding substitute of full EOM-CCSDT. The scaling of the EOM-CC(2,3) model is N^8, the same as of CISDT and EOM-CCSDT.

Amplitudes T satisfy the CCSD equations for the reference state:

$$E_{\mathrm{CC}} = \langle \Phi_0 | \bar{H} | \Phi_0 \rangle, \tag{10}$$

$$\langle \Phi_i^a | \bar{H} - E | \Phi_0 \rangle = 0, \quad \langle \Phi_{ij}^{ab} | \bar{H} - E | \Phi_0 \rangle = 0, \tag{11}$$

and $\bar{H}$ assumes the following form in the basis of the reference, singly, doubly, and triply excited determinants:

$$\bar{H} = \begin{pmatrix} E_{\mathrm{CC}} & \bar{H}_{\mathrm{OS}} & \bar{H}_{\mathrm{OD}} & 0 \\ 0 & \bar{H}_{\mathrm{SS}} & \bar{H}_{\mathrm{SD}} & \bar{H}_{\mathrm{ST}} \\ 0 & \bar{H}_{\mathrm{DS}} & \bar{H}_{\mathrm{DD}} & \bar{H}_{\mathrm{DT}} \\ \bar{H}_{\mathrm{TO}} & \bar{H}_{\mathrm{TS}} & \bar{H}_{\mathrm{TD}} & \bar{H}_{\mathrm{TT}} \end{pmatrix}, \tag{12}$$

where E_{CC} is the reference CC energy and $\bar{H}_{\mathrm{SO}}=\bar{H}_{\mathrm{DO}}=0$ in virtue of CC Eqs. (10) and (11). Due to different truncation levels of T and $R(k)$, the effective Hamiltonian matrix element $\bar{H}_{\mathrm{TO}}$ associated with triply excited determinant $|\Phi_{ijk}^{abc}\rangle$ is nonvanishing, and, consequently, the reference determinant $|\Phi_0\rangle$ is no longer an eigenstate of $\bar{H}$ in the subspace of singly, doubly, and triply excited determinants. The $\bar{H}_{\mathrm{OT}}$ matrix element is zero because the maximum excitation level of Hamiltonian is two.

Since in EOM-CC(2,3) the order of truncation of the cluster operator T is 2, as in EOM-CCSD, the elements of Hamiltonian up to $\bar{H}_{\mathrm{DD}}$ block are identical in these two models. Therefore, the implementation of EOM-CC(2,3) only requires inclusion of the matrix elements involving triple excitations. The EOM-CC(2,3) $\bar{H}$ should be diagonalized in the basis of zero, single, double, and triple excitations. However, in the SF variant of EOM-CC(2,3), the reference is not present in the final EOM states (i.e., $R_0=0$ for all the EOM-SF states), and $\bar{H}$ is diagonalized in the basis of single, double, and triple excitations only.

After subtracting the reference energy from $\bar{H}$, the EOM-CC(2,3) right eigenproblem reads as follows:

$$\begin{aligned} &\begin{pmatrix} 0 & \bar{H}_{\mathrm{OS}} & \bar{H}_{\mathrm{OD}} & 0 \\ 0 & \bar{H}_{\mathrm{SS}} - E_{\mathrm{CC}} & \bar{H}_{\mathrm{SD}} & \bar{H}_{\mathrm{ST}} \\ 0 & \bar{H}_{\mathrm{DS}} & \bar{H}_{\mathrm{DD}} - E_{\mathrm{CC}} & \bar{H}_{\mathrm{DT}} \\ \bar{H}_{\mathrm{TO}} & \bar{H}_{\mathrm{TS}} & \bar{H}_{\mathrm{TD}} & \bar{H}_{\mathrm{TT}} - E_{\mathrm{CC}} \end{pmatrix} \begin{pmatrix} R_0(k) \\ R_1(k) \\ R_2(k) \\ R_3(k) \end{pmatrix} \\ &= \omega_k \begin{pmatrix} R_0(k) \\ R_1(k) \\ R_2(k) \\ R_3(k) \end{pmatrix}, \end{aligned} \tag{13}$$

where ω_k is the energy difference between the coupled-cluster reference energy and the energy of the kth excited state: $\omega_k=E_k-E_{\mathrm{CC}}$. For energy calculations, it is sufficient to solve the right eigenvalue problem only. However, both right and left eigenvectors are required for properties and gradient calculations. Programmable equations and implementation details are given in the Appendix.

B. Active space EOM-CC(2,3) model

To reduce computational costs and to extent the scope of the problems amendable to the EOM-CC(2,3) treatment, we implemented an active space variant of EOM-CC(2,3), EOM-CC(2,$\widetilde{3}$). We start by dividing all spin orbitals into O core (restricted occupied) spin orbitals ($\mathbf{i}$, $\mathbf{j}$, $\mathbf{k}$),$\mathbf{O}$ active occupied spin orbitals ($\mathbf{I}$, $\mathbf{J}$, $\mathbf{K}$),$\mathbf{V}$ active unoccupied spin orbitals ($\mathbf{A}$, $\mathbf{B}$, $\mathbf{C}$), and V restricted virtual spin orbitals ($\mathbf{a}$, $\mathbf{b}$, $\mathbf{c}$), all relative to $|\Phi_0\rangle$. Our implementation of the active space model is defined as follows:

$$T = T_1 + T_2, \tag{14}$$

$$R'(k) = R_0(k) + R_1(k) + R_2(k) + r_3(k), \tag{15}$$

where all the excitation operators are defined as usual, except for $r_3(k)$, which is defined as

$$r_3(k) = r_{\mathbf{I}jk}^{ab\mathbf{C}}(k), \tag{16}$$

that is, all T amplitudes and $R_{1,2}(k)$ are defined in the full space, whereas only internal and semi-internal triple excitations are present in $R'(k)$. The excitation energies are defined by solving a set of equations (13), in which the active space $R'(k)$ operator and triexcited determinant $|\Psi_{\mathbf{I}jk}^{ab\mathbf{C}}\rangle$ substitute the full space $R(k)$ and $|\Psi_{ijk}^{abc}\rangle$. The number of these semi-internal triples is $\mathbf{O}\mathbf{V}O^2V^2$, i.e., the prefactor times the number of doubles.

As with any active space method, the thoughtful choice of the active space for EOM-CC(2,$\widetilde{3}$) is crucial for obtaining accurate excitation energies. For valence states, the most straightforward but prohibitively expensive choice is to include all valence orbitals. Fortunately, as shown in Sec. III, using much smaller active spaces can be sufficient. In general, the active space should include: (i) orbitals that describe the leading character of a target state (later referred to as the minimal active space) and (ii) orbitals that contribute to the spin-contamination, symmetry breaking, or other problems of the reference or target states. Selecting orbitals of type (i) is straightforward; e.g., these are singly occupied orbitals in radicals, (nearly)-degenerate diradical or triradical orbitals, and so on. Choosing orbitals of type (ii) is more ambiguous. Analysis of the T and R amplitudes from a separate EOM-CCSD calculation is often needed for that purpose. Often, the problematic orbitals appear in $R(k)$ or T amplitudes with considerable weights; i.e., these are orbitals that contribute to the multiconfigurational nature of the reference and/or excited states. In some cases, there is no need in orbitals of type (ii), e.g., see the methylene example from Sec. III B, whereas in others, e.g., see Sec. III D, omitting orbitals of type (ii) can significantly affect the results.

Overall, the inclusion of semi-internal triples results in significant improvements when non-dynamical correlation is important. However, full triples are needed to accurately recover the dynamical correlation. Overall, the accuracy of EOM-CC(2,$\widetilde{3}$) will differ from that of full EOM-CC(2,3) by the value of the dynamical correlation correction recovered by the triple excitations. Based on our benchmarks, this value is usually less than 0.1 eV.

Our active space EOM model is similar to that implemented in Refs. 16, 17, 34, and 35 and to the approach of Szalay and Gauss, who augmented single and double EOM excitations by a selection of semi-internal triples recovering the spin symmetry of the excited state, i.e., the so called pseudo-triple excitations.

C. Size-extensivity of EOM-CC(2,3)

In this section, we discuss the size-extensivity of the EOM-EE-CC(2,3) and EOM-SF-CC(2,3) models, closely following the presentation from Refs. 36 and 37. We adhere to the terminology used in Refs. 36 and 38 and use the term "size-extensivity" to refer to the additive separability of the energy in the limit of noninteracting fragments:

$$E_{AB} = E_A + E_B, \tag{17}$$

where E_{AB} is the energy of a system composed of two noninteracting fragments, A and B, at infinite separation and E_A, E_B are energies of the corresponding fragments. Here, we restrict ourselves to the case when A and/or B are closed-shell systems. For the EOM-CC(2,3) models, the total energy of a target state consists of the reference energy and the corresponding transition energy. Thus, Eq. (17) is satisfied if (i) the reference energy of the composite system is the sum of the reference energies for fragments and (ii) the transition energy is additive. Condition (i) is satisfied by any EOM-CC model due to the size-extensivity of the coupled-cluster model for cases when either both fragments are closed-shell molecules or for a closed-shell and an open-shell fragment, provided that the UHF orbitals are employed.

Below we show that for EOM-SF-CC(2,3), the transition energy for the "excitation" localized on fragment A in the supermolecule is the same as the transition energy for the isolated fragment A, i.e., the energies of target states on the fragment A are not affected by the presence (at infinite distance) of the fragment B. Thus, the quality of the EOM-SF-CC(2,3) description would not degrade with the increase of molecular size. The EOM-EE-CC(2,3) model, however, is not fully size-extensive because the transition energy between the reference and the excited state in EOM-EE-CC(2,3) is not additive. However, the *transition energies* between the EOM-EE-CC(2,3) excited states *are* additive. Thus, EOM-EE-CC(2,3) exhibits limited size-extensivity.

We start by dividing all the determinants into four groups: (i) the reference determinant, $|0_A \cdot 0_B\rangle$ or simply $|0\rangle$; (ii) determinants involving excitations localized on fragment A, $|\Phi_A \cdot 0_B\rangle$ or $|A\rangle$; (iii) determinants involving excitations localized on fragment B,$|0_A \cdot \Phi_B\rangle$ or $|B\rangle$; and (iv) determinants that involve excitations of electrons on both fragments, $|\Phi_A \cdot \Phi_B\rangle$ or $|AB\rangle$ (i.e., those describing simultaneous excitations of both subsystems or electron transfer between them).

In the SF implementation employing a triplet reference, the reference determinant is the CC solution describing the $\alpha\alpha$ component of the reference triplet state. Without loss of generality, we assume that the two unpaired α electrons are localized on fragment A. Thus, for EOM-SF, $|0_A\rangle$ is the CC wave function for fragment A in the *triplet* state and $|0_B\rangle$ is the CC wave function for fragment B in the *singlet* state.

Later in the discussion, we use $|0\rangle$ and $|\mathbf{p}\rangle$ to refer to (i) and (ii)–(iv) determinants, respectively. While $|0\rangle$ is the $M_s=1$ determinant, all $|\mathbf{p}\rangle$ have $M_s=0$, since they are generated by spin-flipping excitations from $|0\rangle$.

In the separated limit, the Hamiltonian operator (and the similarity transformed Hamiltonian[39] as well) of the composite system is the sum of those for the individual fragments:

$$\bar{H} = \bar{H}_A + \bar{H}_B. \tag{18}$$

As pointed out by Koch *et al.*,[40] the sufficient condition for size-extensivity is an upper-triangle structure of the matrix of the Hamiltonian (18) in the many-electron basis described above, which ensures that eigenvalues of the composite Hamiltonian $\bar{H}_{AB}$ *include* eigenvalues of $\bar{H}_A$ and $\bar{H}_B$.

For EOM-CC(2,3), the matrix of the Hamiltonian (18) has the following form in the above basis:

$$H = \begin{pmatrix} \bar{H}_{00} & \bar{H}_{0A} & \bar{H}_{0B} & \tilde{0} \\ \bar{H}_{A0} & \bar{H}_{AA} & \tilde{0} & \bar{H}_{A,AB} \\ \bar{H}_{B0} & \tilde{0} & \bar{H}_{BB} & \bar{H}_{B,AB} \\ \tilde{0} & \mathbf{0} & \mathbf{0} & \bar{H}_{AB,AB} \end{pmatrix}, \tag{19}$$

where the shorthand notation $\bar{H}_{PQ} \equiv \langle P|\bar{H}|Q\rangle$ has been used. The $\bar{H}_{AB}, \bar{H}_{BA}, \bar{H}_{0,AB}$, and $\bar{H}_{AB,0}$ blocks, i.e., tilded zeros $\tilde{0}$ from Eq. (19), involve only matrix elements of the Hamiltonian, which couple subsystems A and B and vanish in the separated limit:[38]

$$\begin{aligned} \bar{H}_{AB} &= \langle \Phi_A \cdot 0_B | \bar{H}_A + \bar{H}_B | 0_A \cdot \Phi_B \rangle \\ &= \langle 0_B | \Phi_B \rangle \cdot \langle \Phi_A | \bar{H}_A | 0_A \rangle + \langle \Phi_A | 0_A \rangle \cdot \langle 0_B | \bar{H}_B | \Phi_B \rangle \\ &= 0 \cdot \langle \Phi_A | \bar{H}_A | 0_A \rangle + 0 \cdot \langle 0_B | \bar{H}_B | \Phi_B \rangle = 0. \end{aligned} \tag{20}$$

The boldface zeros in Eq. (19) vanish as a result of the coupled-cluster condition $\langle \mathbf{p}|\bar{H}|0\rangle = 0$, where $|\mathbf{p}\rangle$ includes single and double excitations only, i.e., the H_{OS} and H_{OD} blocks in Eq. (12) are zero. For example, for the $\bar{H}_{AB,A}$ element,

$$\begin{aligned} \bar{H}_{AB,A} &= \langle \Phi'_A \cdot \Phi_B | \bar{H}_A + \bar{H}_B | \Phi_A \cdot 0_B \rangle \\ &= \langle \Phi_B | 0_B \rangle \cdot \langle \Phi'_A | \bar{H}_A | \Phi_A \rangle + \langle \Phi'_A | \Phi_A \rangle \cdot \langle \Phi_B | \bar{H}_B | 0_B \rangle \\ &= \langle \Phi'_A | \Phi_A \rangle \cdot \langle \Phi_B | \bar{H}_B | 0_B \rangle = 0. \end{aligned} \tag{21}$$

The last statement is true because in the $|\Phi'_A \cdot \Phi_B\rangle$ determinant, Φ_A includes *at least* one electron excitation, and the excitation level in the determinant Φ_B does not exceed *doubly excited* substitutions.

Thus, the only elements that might prevent Hamiltonian (19) from having the upper-triangle form, and thus affect the size-extensivity, are $\bar{H}_{A0}$ and $\bar{H}_{B0}$. Further analysis reveals that $\bar{H}_{A0}$ does not break the size-extensivity because this matrix element couples only $|0\rangle$ and $|A\rangle$ determinants, which are already coupled in the EOM-CC(2,3) equations for the monomer. $\bar{H}_{B0}$ is zero for the SF variant of EOM-CC(2,3) because, as discussed in Sec. II A, the $\bar{H}_{TO}$ matrix element of Hamiltonian is zero for EOM-SF-CC(2,3) [see Eq. (12)]. Thus, the EOM-SF-CC(2,3) model is size-extensive. However, this is true only if one employs *unrestricted Hartree-Fock triplet or quartet orbitals* for the reference determinant. In the case of *restricted* triplet or quartet orbitals, the EOM-SF-CC(2,3) model, as well as any ground-state ROHF-based CC model, includes (numerically small) terms violating size-extensivity.

Contrary to EOM-SF-CC(2,3), the EOM-EE-CC(2,3) $\bar{H}_{B0}$ is not zero due to the nonvanishing $\langle \Phi^{abc}_{ijk}|\bar{H}|\Phi_0\rangle$ matrix element [see Eq. (12)]. Thus, the EOM-EE-CC(2,3) model is not size-extensive. However, the $\bar{H}_{TO}$ element is not zero only for the EOM amplitudes of the reference state and the excited states of the same spin and spatial symmetry as the reference state; in all other excited states R_0, and, consequently, $\bar{H}_{TO}$ are zero. For the excited states of the same spin and spatial symmetry as the reference state, the $\bar{H}_{TO}$ matrix element is not zero; however, its contribution to excitation energy is small, unless an excited state is degenerate with the reference (e.g., $^2\Pi$ radicals). As a result, the transition energies between almost any two EOM target states are size-extensive or nearly size-extensive.

Since the size-extensivity of EOM-EE(2,3) is violated by the CI-type improvement of the reference state due to triple excitations, the problem could be avoided by excluding the $|\Phi_0\rangle$ block from the EOM-CC(2,3) eigenvalue problem. However, this would result in unbalanced description of the reference and the target EOM states. The resulting excitation energies will be systematically underestimated with respect to the EOM-EE-CC(2,3) ones; however, the relative separations between the EOM states of the symmetry different than that of the reference will remain the same (see Table I for an example). Based on our calculations, the triples correction for the reference ranges from a thousandth of eV (see the Be example in Table I) to up to 1 eV for systems with poor or spin-contaminated references, the typical value being 0.1–0.2 eV.

Interestingly, both EE and SF variants of the active space EOM-CC(2,3) model *are* size-extensive. Whereas the size-extensivity of EOM-SF is not surprising, a comment is required on the size-extensivity of EOM-EE-CC(2,$\tilde{3}$). The problematic element of full space EOM-EE-CC(2,3), H_{B0}, becomes zero for EOM-SF-CC(2,$\tilde{3}$) since, with active space being localized on the fragment A, there are no triple excitations on the fragment B.

Table I presents a numerical example, which demonstrates the size-extensivity issues for EOM-SF-CC(2,3) and EOM-EE-CC(2,3) for a Be atom with a Ne atom located 100 Å away. For a size-extensive method, the excitation energies of Be will not be affected by the presence of Ne. This is indeed the case for EOM-SF-CC(2,3), EOM-SF-CC(2,$\tilde{3}$), and EOM-EE-CC(2,$\tilde{3}$). However, for EOM-EE-CC(2,3), the EOM energy of the target $^1S(1s^2 2s^2)$ state is affected by Ne. This is because the EOM energy of the reference state is affected mostly by the $\bar{H}_{TO}$ matrix element, which breaks the size-extensivity of EOM-EE-CC(2,3). $\bar{H}_{TO}$ is also nonzero for the second ^1S state. However, as expected, the violation

TABLE I. The EOM-EE-CC(2,3) and EOM-SF-CC(2,3) ground state reference (hartree) and excitation (eV) energies for the Be atom with and without a Ne atom 100 Å away. 6-31G basis set. The excitation energies are given with respect to the energy of the reference state, i.e., for example, the real excitation energies of Be by EOM-SF-CC(2,3) are $E_{3P(1s^22s2p)}=2.8616$ eV, $E_{1P(1s^22s2p)}=6.5774$ eV, $E_{3P(1s^22p_x2p_{x,y})}=7.6689$ eV, and $E_{1D(1s^22p^2)}=8.6245$ eV.

Method	System	Reference[a]	^1S $(1s^22s^2)$	^3P[b] $(1s^22s2p)$	^1P[b] $(1s^22s2p)$	^3P $(1s^22p_x2p_{x,y})$	^1D[b] $(1s^22p^2)$	^1S $(1s^22p^2)$
EOM-EE-CC(2,3)	Be	−14.613518	−0.0006	2.8608	6.5767		8.6241	10.9514
EOM-EE-CC(2,3)	Be–Ne	−143.202513	−0.0201	2.8608	6.5767		8.6241	10.9514
EOM-EE-CC(2,$\tilde{3}$)[c]	Be	−14.613518	−0.0006	2.8609	6.5767		8.6241	10.9515
EOM-EE-CC(2,$\tilde{3}$)[c]	Be–Ne	−143.202513	−0.0006	2.8609	6.5767		8.6241	10.9515
EOM-SF-CC(2,3)	Be	−14.508385	−2.8616	0.0000	3.7158	4.8073	5.7629	8.0899
EOM-SF-CC(2,3)	Be–Ne	−143.097379	−2.8616	0.0000	3.7158	4.8073	5.7629	8.0899
EOM-SF-CC (2,$\tilde{3}$)[c]	Be	−14.508385	−2.8615	0.0000	3.7159	4.8074	5.7630	8.0900
EOM-SF-CC (2,$\tilde{3}$)[c]	Be–Ne	−143.097379	−2.8615	0.0000	3.7159	4.8074	5.7630	8.0900

[a]The CCSD energy of the ^1S state for EOM-EE-CC(2,3) and of the ^3P state for EOM-SF-CC(2,3).
[b]At the EOM-SF-CC(2,3) level, these states regained the degeneracy.
[c]The active space consists of the valence $2s$ and $2p_x, 2p_y, 2p_z$ orbitals of Be.

of the size-extensivity for this state is much smaller than for the reference state; e.g., for the Be–Ne example, it is less than 0.0001 eV. For all other excited states from Table I, the excitation energies with respect to the reference state are size- extensive.

III. RESULTS AND DISCUSSION

Hirata *et al.*[5] benchmarked EOM-EE-CC(2,3), as well as other EOM-EE-CC models, on the excited states of CH^+ using the closed-shell references. Our study extends the benchmark set by including the following open-shell systems: (i) two problematic radicals, CH and CO^+; (ii) the CH_2 diradical; (iii) the trimethylenemethane (TMM) diradical; and (iv) the dehydro-meta-xylylene (DMX) triradical. For the latter two systems, we employed an extrapolation technique based on an energy separability scheme[26] to obtain EOM-CC(2,3) results apt for comparison with experiment:

$$E^{\text{large}}_{\text{EOM-CC(2,3)}} = E^{\text{small}}_{\text{EOM-CC(2,3)}} + (E^{\text{large}}_{\text{EOM-CCSD}} - E^{\text{small}}_{\text{EOM-CCSD}}), \tag{22}$$

where E^{large} and E^{small} refer to the total energies calculated in large (e.g., cc-pVTZ) and small (e.g., 6-31 G*) basis sets. This procedure assumes that changes in the total energy due to the basis set increase are similar for the less and more correlated models [e.g., MP2 and CCSD or EOM-CCSD and EOM-CCSD(2,3)].

Our benchmark study addresses the following questions: (i) the extent of the effect of spin-contamination on the accuracy of EOM-CC(2,3), (ii) the sensitivity of EOM-CC(2,3) to a choice of the reference (UHF versus ROHF), and (iii) the choice of the active space and accuracy of EOM-CC(2,$\tilde{3}$).

All calculations were performed using the Q-CHEM[41] electronic structure package, to which our EOM-CC(2,3) codes are interfaced. To validate the EOM-CC(2,$\tilde{3}$) implementation, the calculations using the DETCI code[42,43] from PSI 3 (Ref. 44) were performed.

A. CO^+ and CH radicals

Due to their challenging electronic structure, the CH and CO^+ radicals have been extensively studied.[20,21,45] To compare the EOM-CC(2,3) data against the multireference configuration interaction (MRCI) results from Ref. 20 and against spin-restricted LRT-CCSD[20] and CC3,[21] we performed calculations in the Sadlej-pVTZ (PBS) basis set[46,47]

TABLE II. Total energies of the ground state (hartree) and vertical excitation energies (eV) of the two low-lying excited states of CO^+ calculated using different EOM-CC methods with ROHF and UHF references. Calculations performed at the experimental ground-state geometry (Ref. 48), $\mathbf{r}$(CO)=1.115 Å using the PBS and 6-311G* basis sets with frozen core orbitals.

Method	$\tilde{X}\,^2\Sigma^+$	$A\,^2\Pi$	$B\,^2\Sigma^+$
PBS basis			
UHF-EOM-EE-CCSD	−112.566265	3.533	6.199
ROHF-EOM-EE-CCSD	−112.566036	3.230	6.011
UHF-EOM-EE-CC(2,3)	−112.579033	3.369	5.890
ROHF-EOM-EE-CC(2,3)	−112.579096	3.353	5.866
SR-CCSD[a]		3.22	6.07
UHF-CC3[b]		3.330	5.811
ROHF-CC3[b]		3.290	5.725
MRCI		3.30	5.88
6-311G* basis			
UHF-EOM-EE-CCSD	−112.576060	3.577	6.189
UHF-EOM-EE-CC(2,$\tilde{3}$)[c]	−112.587836	3.375	5.851
UHF-EOM-EE-CC(2,3)	−112.590873	3.403	5.871
ROHF-EOM-EE-CCSD	−112.575807	3.265	5.992
ROHF-EOM-EE-CC(2,$\tilde{3}$)[c]	−112.590921	3.389	5.846
ROHF-EOM-EE-CC(2,3)	−112.588033	3.345	5.808
Experiment[d]		3.264	5.819

[a]Reference 20.
[b]Reference 21.
[c]EOM-CC(2,$\tilde{3}$) with six-orbital active space; see text for details.
[d]Experimental results as reported in Ref. 45.

TABLE III. Total energies of the ground state (hartree) and vertical excitation energies (eV) of several low-lying excited states of CH radical calculated using various CC methods with ROHF and UHF references. Calculations performed at the experimental ground state geometry (Ref. 48), $r(\mathrm{CH})=1.1198$ Å, using the PBS basis set with one frozen core orbital.

Method	$X\,^2\Pi$	$X\,^2\Pi$ (EOM)[a]	$a\,^4\Sigma^-$	$A\,^2\Delta$[b]	$A\,^2\Delta$[c]	$B\,^2\Sigma^-$	$C\,^2\Sigma^+$
UHF-EOM-EE-CCSD	−38.385379	0.011	0.944	3.221	3.331	4.404	5.312
ROHF-EOM-EE-CCSD	−38.385681	0.005	0.908	3.215	3.304	4.230	5.199
UHF-EOM-EE-CC(2,3)	−38.388600	0.011	0.659	3.030	3.026	3.328	4.107
ROHF-EOM-EE-CC(2,3)	−38.388582	0.010	0.654	3.023	3.022	3.325	4.102
UHF-EOM-SF-CCSD	−38.386340	0.0	0.624	3.030	3.030	3.341	4.114
ROHF-EOM-SF-CCSD	−38.363525	0.0	0.625	3.025	3.025	3.347	4.108
UHF-EOM-SF-CC(2,3)	−38.388101	0.0	0.636	3.000	3.000	3.316	4.056
ROHF-EOM-SF-CC(2,3)	−38.388143	0.0	0.636	2.999	2.999	3.318	4.055
CCSD-psT-LRT[d]				3.14		3.48	5.16
UHF-CC3[e]				3.173		3.643	4.517
ROHF-CC3[e]				3.160		3.576	4.472
MRCI				2.96		3.31	4.03
Experiment (adiabatic)[f]			0.725	2.875		3.229	3.943
Experiment (vertical)[g]			0.745	2.880		3.263	3.943

[a]The energy of the $X\,^2\Pi$ state found in the EOM procedure (see text).
[b]The open-shell component of the $A\,^2\Delta$ state.
[c]The closed-shell component of the $A\,^2\Delta$ state.
[d]Reference 20.
[e]Reference 21.
[f]Reference 48.
[g]Estimated from the adiabatic excitation energies within the harmonic approximation for the excited state PES using experimental data (Ref. 48).

with frozen core orbitals. These data are shown in Tables II and III. To investigate the performance of EOM-CC$(2,\widetilde{3})$, we performed additional sets of calculations in the non-diffuse 6-311G* (Ref. 49) (CO^+) and cc-pVTZ (Ref. 50) (CH) bases.[51] These results are reported in Tables II and IV.

CO^+ is a radical with the considerably spin-contaminated reference and, consequently, spin-contaminated excited states. As shown in Table II, the spin-contamination manifests itself in large differences between the UHF-EOM-CCSD and ROHF-EOM-CCSD excitation energies (0.2–0.3 eV). However, for EOM-CC(2,3), there is only a small difference (~0.02 eV) between the ROHF and UHF values. A similar behavior, i.e., a significant reduction of spin-contamination with inclusion of triple excitations, was previously reported for other models with triple excitations, e.g., CC3.[21] For CO^+, the accuracy of EOM-CC(2,3) exceeds that of SR-CCSD-LRT and is similar to the accuracy of CC3; the differences between EOM-CC(2,3) and MRCI results do not exceed 0.07 eV.

As an active space for the $^2\Pi$ and $^2\Sigma^+$ valence states of CO^+, we chose the following set of orbitals: $4a_1^2, 1b_1^2, 1b_2^2, 5a_1^1, 2b_1^0, 2b_2^0$; i.e., in addition to singly-occupied $5a_1^1$, we augmented the active space by three highest doubly occupied and two lowest virtual orbitals. These orbitals are shown in Fig. 1. The $4a_1^2, 1b_1^2, 1b_2^2$, and $5a_1^1$ orbitals form the minimal active space for the $^2\Pi$ and $^2\Sigma^+$ states (see Sec. II B), whereas $2b_1^0$ and $2b_2^0$ were added as orbitals being next important for the description of these states. The importance of these orbitals was derived from the analysis of the EOM-CCSD wave functions, which revealed large excitation amplitudes involving these two virtual orbitals.

From Table II, EOM-CC$(2,\widetilde{3})$ is a definite improvement over EOM-CCSD, and the differences between active space and full EOM-CC(2,3) values do not exceed 0.05 eV.

The electronic structure of the CH radical is described in Fig. 2. From the methodological point of view, CH is a triradical, as it features three electrons distributed over three nearly degenerate orbitals ($3a_1, 1b_1$, and $1b_2$ in C_{2v} symmetry group notations). Slater determinants that can be generated by distributing three electrons over three orbitals are shown in Fig. 3. The lowest electronic states of CH are given in the right panel of Fig. 2. The ground state of CH, a doubly degenerate $^2\Pi$ state, is closely followed by the $^4\Sigma^-$ quartet state. About 3 eV higher lies the $^2\Delta$ state (one of its components is of a "closed-shell" type, and another is of an "open-shell" type). Slightly higher is the "open-shell" $^2\Sigma^-$ doublet, and, finally, there is the $^2\Sigma^+$ state.

Table III summarizes vertical excitation energies of CH calculated by different CC methods. Clearly, using the ground state wave function as a reference for EOM-CC leads to intrinsic problems in the description of many if not all excited states, since only one component of the $^2\Pi$ state ($3a_1^2, 1b_1^1$ or $3a_1^2, 1b_2^1$) is used as a reference determinant. As a result, the second component of this state appears as an EOM state [column $X\,^2\Pi$ (EOM) in Table III]; i.e., the degeneracy between the two components of $^2\Pi$ is not reproduced. Another problem arises with the electronic states, which include

TABLE IV. Total energies of the ground state (hartree) and vertical excitation energies (eV) of several low-lying excited states of CH radical calculated using the active space EOM-EE-CC(2,3) and EOM-SF-CC(2,3) methods with ROHF and UHF references. Calculations performed at the experimental ground state geometry (Ref. 48), r(CH)=1.1198 Å, using the cc-pVTZ basis set with one frozen core orbital.

Method	$X\,^2\Pi$	$X\,^2\Pi$ (EOM)[a]	$a\,^4\Sigma^-$	$A\,^2\Delta$[b]	$A\,^2\Delta$[c]	$B\,^2\Sigma^-$	$C\,^2\Sigma^+$
UHF-EOM-EE-CCSD	−38.407096	0.015	1.024	3.210	3.223	4.590	5.521
UHF-EOM-EE-CC(2,$\tilde{3}$)[d]	−38.408764	0.009	0.751	3.031	3.021	3.356	4.156
UHF-EOM-EE-CC(2,3)	−38.411018	0.017	0.743	3.009	3.004	3.343	4.113
ROHF-EOM-EE-CCSD	−38.406975	0.007	0.991	3.205	3.295	4.402	5.402
ROHF-EOM-EE-CC(2,$\tilde{3}$)[d]	−38.408772	0.001	0.723	3.000	3.010	3.342	4.141
ROHF-EOM-EE-CC(2,3)	−38.410986	0.016	0.738	3.000	2.998	3.340	4.117
UHF-EOM-SF-CCSD	−38.407473	0.0	0.687	2.991	2.991	3.343	4.118
UHF-EOM-SF-CC(2,$\tilde{3}$)[d]	−38.408372	0.0	0.697	2.964	2.964	3.325	4.070
UHF-EOM-SF-CC(2,3)	−38.410184	0.0	0.709	2.965	2.965	3.332	4.056
Experiment (adiabatic)[e]			0.725	2.875		3.229	3.943
Experiment (vertical)[f]			0.745	2.880		3.263	3.943

[a]The energy of the $X\,^2\Pi$ state found in the EOM procedure.
[b]The open-shell component of the $A\,^2\Delta$ state.
[c]The closed-shell component of the $A\,^2\Delta$ state.
[d]Active space EOM-CC(2,3) with three-orbital active space; see text for detail.
[e]Reference 48.
[f]Estimated from the adiabatic excitation energies within the harmonic approximation for the excited state PES using experimental data (Ref. 48).

configurations that are formally doubly excited with respect to the reference, e.g., configurations (3) and (10) from Fig. 3. Configuration (3) is a so-called pseudodouble excitation with respect to the reference determinant [configuration (5)]; it appears in the quartet $^4\Sigma^-$, in the open-shell component of the $^2\Delta$ state, and in the $^2\Sigma^-$ doublet. Configuration (10) contributes to the closed-shell component of the $^2\Delta$ state, in which the weight of this configuration is not very large, and to the $^2\Sigma^+$ state, where configuration (10) is dominant. Thus, all these states (excluding, perhaps, the closed-shell component of $^2\Delta$) are expected to suffer from unbalanced description by any EOM-CC model, which employs the ground state as a reference. Inclusion of triples (or quadruples) will reduce but not fully eliminate this intrinsic imbalance.

From Table III, both UHF and ROHF based EOM-CCSD fail to describe $^2\Sigma^-$ and $^2\Sigma^+$ states. Two components of the $^2\Delta$ state, which lost their degeneracy due to different excitation levels of leading configurations, and the $^4\Sigma^-$ quartet are about 0.2–0.3 eV off relative to the MRCI results. EOM-CC(2,3) dramatically improves the description. For all the states considered, the largest deviation from the MRCI results is 0.08 eV. Differences between the UHF and ROHF data are less than 0.01 eV. For CH, EOM-CC(2,3) performs much better than the CCSD-psT-LRT or CC3 methods.

As expected, EOM-CC(2,3) does not fully restore the degeneracy between different components of the multicomponent states ($^2\Pi$ and $^2\Delta$). An alternative (and methodologically correct) way to treat this problem is by using the SF rather than the EE variant of EOM-CC. As demonstrated in Refs. 52 and 53, EOM-SF-CCSD accurately describes all triradical states by employing the high-spin component of the quartet state as a reference. As a result, even EOM-SF-CCSD results are in excellent agreement with MRCI ones (discrepancies are less than 0.1 eV), the EOM-SF-CC(2,3) data further improving. As an important consequence of using the method that provides the balanced description of the

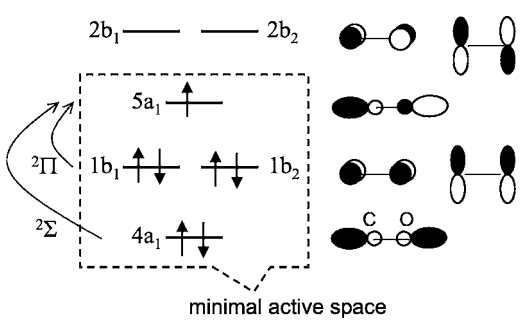

FIG. 1. Electronic structure of CO^+ radical. Orbital labels are given in C_{2v} symmetry group. The two lowest excited states of CO^+ are dominated by excitations from the $4a_1^2$ and $1b_1^2/1b_2^2$ to $5a_1^1$ orbital. Thus, these orbitals form the minimal active space for the EOM-CC(2,$\tilde{3}$) calculations. Inclusion of the antibonding π orbitals in the active space is also important.

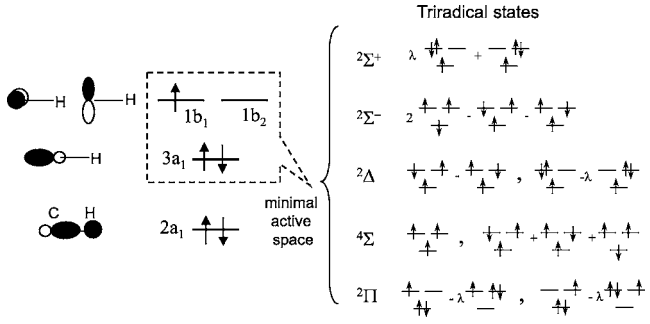

FIG. 2. Electronic structure of the CH (tri)radical. Orbital labels are given in the C_{2v} symmetry group. Distribution of three electrons in $3a_1, 1b_1$, and $1b_2$ triradical orbitals results in a number of low-lying electronic states shown on the right. EOM-CC(2,$\tilde{3}$) with the active space composed of these three orbitals yields accurate results.

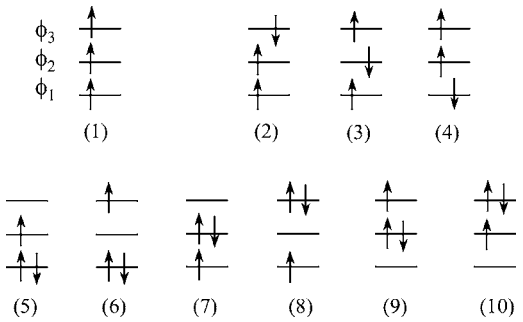

FIG. 3. Slater determinants that can be generated by distributing three electrons over three orbitals. Only determinants with a positive projection of the total spin are shown. Determinant (1) has $M_s=3/2$, determinants (2)–(10) have $M_s=1/2$. We refer to determinants (2)–(4) and to states including these determinants as of open-shell type, whereas determinants (5)–(10) are of closed-shell type.

excited states, the multicomponent states appear as *fully degenerate* both in EOM-SF-CCSD and EOM-SF-CC(2,3). Moreover, the spin-contamination of SF states is very small even at the EOM-SF-CCSD level—the UHF and ROHF data differ by less than 0.01 eV.

The EOM-CC(2,$\tilde{3}$) results are shown in Table IV. As an active space for both the EE and SF variants of EOM-CC(2,3), we choose three triradical orbitals ($3a_1, 1b_1, 1b_2$). This is the minimal active space, as all leading excitations occur within these orbitals. For both UHF- and ROHF-based EOM-EE-CC(2,3), this active space yields excellent results: the differences between the active space and full EOM-EE-CC(2,3) are less than 0.05 and 0.03 eV for UHF and ROHF, respectively. For the SF variant, the active space EOM-SF-CC(2,3) also improves the performance of EOM-SF-CCSD and approaches the accuracy of full EOM-SF-CC(2,3)—active space and full EOM-SF-CC(2,3) results differ by less than 0.02 eV. However, the relative improvement of EOM-CC(2,$\tilde{3}$) over EOM-CCSD is more modest for the SF than the EE variant. For example, for the $^2\Sigma^+$ state, EOM-EE-CC(2,$\tilde{3}$) recovers about 1.3 eV of discrepancy between the CCSD and CC(2,3) energies, whereas the corresponding gain of EOM-SF-CC(2,$\tilde{3}$) is only 0.05 eV. This observation does not suggest that the chosen active space is more appropriate for EOM-EE-CC(2,$\tilde{3}$) than for EOM-SF-CC(2,$\tilde{3}$). Rather, we can conclude that (i) the inclusion of semi-internal triples efficiently solves the problem caused by non-dynamical correlation; i.e., the active space improved the EOM-EE-CCSD results corrupted due to orbital degeneracies, and (ii) a small subset of triples was not sufficient to recover the dynamical correlation correction available through using full triples.

B. CH_2 diradical

The CH_2 diradical is a popular benchmark system.[54–57] Following our benchmark study,[58] we now investigate how EOM-CC(2,3) improves the performance of the SF and EE variants of EOM-CCSD. We also consider the active space EOM-CC(2,3) and analyze the performance of EOM-EE-CC(2,3), which employs a deliberately poor reference, the *excited* $2\,^1A_1$ determinant.

TABLE V. Total energies of the ground state (hartree) and adiabatic excitation energies (eV) of the CH_2 diradical calculated by different EOM-EE-CC and EOM-SF-CC methods in comparison to the FCI energies. TZ2P basis set from Ref. 54, one frozen core and one frozen virtual orbital; FCI/TZ2P optimized geometries (Ref. 57).

Method	$^3B_1$	$1\,^1A_1$	$^1B_1$	$2\,^1A_1$
EOM-EE-CCSD	−39.063114	0.526	1.565	3.799
EOM-EE-CC(2,$\tilde{3}$)[a]	−39.063163	0.488	1.545	2.757
EOM-EE-CC(2,3)	−39.065456	0.454	1.539	2.689
EOM-EE-CCSD ($2\,^1A_1$ ref)	−39.057717	1.921	1.439	1.894
EOM-EE-CC(2,$\tilde{3}$)[a] ($2\,^1A_1$ ref)	−39.062944	0.692	1.541	2.734
EOM-EE-CC(2,3) ($2\,^1A_1$ ref)	−39.065375	0.657	1.541	2.676
EOM-SF-CCSD[b]	−39.062846	0.510	1.564	2.715
EOM-SF-CC(2,$\tilde{3}$)[a,b]	−39.063078	0.497	1.554	2.705
EOM-SF-CC(2,3)[b]	−39.065208	0.477	1.542	2.664
FCI[c]	39.066738	0.483	1.542	2.674

[a]EOM-CC(2,$\tilde{3}$) with two-orbital active space; see text for details.
[b]UHF reference used for SF calculations.
[c]FCI results from Ref. 57.

Adiabatic excitation energies of CH_2 calculated by EOM-CCSD and EOM-CC(2,3), as well as the FCI results from Ref. 57, are summarized in Table V. Using the $1\,^1A_1$ state as a reference (the EE approach), the triplet $^3B_1$ and the open-shell $^1B_1$ singlet appear as the EOM states with a dominant singly excited character. The discrepancy between EOM-EE-CCSD and FCI for these two states is less than 0.05 eV. However, the second closed-shell $2\,^1A_1$ singlet is dominated by the double excitation from this reference. As a result, the EOM-EE-CCSD description of this state is very poor—the error is more than 1 eV. The SF model treats all four diradical states as the excited spin-flipped states from the high-spin triplet reference determinant. Consequently, all the above states have a dominant singly excited character and are described by EOM-SF-CCSD in a balanced way—errors against FCI are less than 0.04 eV.

EOM-CC(2,3) represents an improvement over both EE-EOM and SF-EOM—the errors against FCI are 0.03 and 0.01 eV, respectively.

As the minimal active space for the EOM-CC(2,3), we choose two diradical orbitals, $3a_1$ and $1b_1$. From Table V, the accuracy of EOM-CC(2,$\tilde{3}$) closely follows that of EOM-CC(2,3)—errors against FCI are less than 0.1 and 0.03 eV for EE and SF variants, respectively.

To test how robust EOM-EE-CC(2,3) is with respect to the reference choice, we calculated the electronic states of CH_2 starting from the *excited* $2\,^1A_1$ reference determinant. As shown in Table V, EOM-CCSD fails to describe both the $1\,^1A_1$ and $2\,^1A_1$ closed-shell singlets. The results of EOM-CC(2,3) are much better—the $^1B_1$ and $2\,^1A_1$ states are in excellent agreement with FCI; the $1\,^1A_1$ state is only 0.18 eV off. The active space variant also performs well; e.g., the EOM-CC(2,$\tilde{3}$) energies are within 0.06 eV from the EOM-CC(2,3) values. To conclude, the inclusion of triples in EOM-CC(2,3) dramatically improves the EOM-CCSD energies even when a poorly described state is used as a refer-

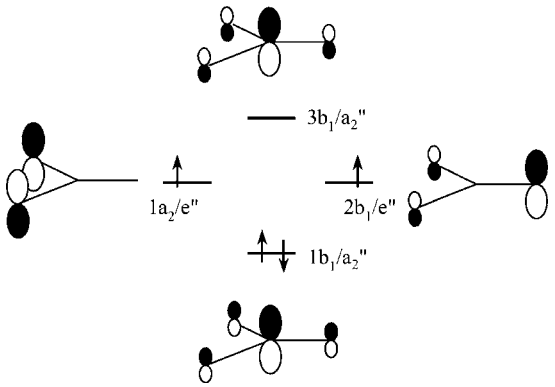

FIG. 4. The π system of TMM at the D_{3h} geometry (C_{2v} symmetry labels are also given). Distribution of two electrons in two diradical orbitals ($2b_1$ and $1a_2$) determines the electronic state of TMM. Thus, this is the minimal active space for EOM-SF-CC(2,$\tilde{3}$). However, inclusion of two other π orbitals in active space is also important.

ence; the small but correctly selected active space gives accurate results as well.

C. TMM

For more than 50 years TMM attracts attention of both experimentalists and theoreticians.[59–65] In this fascinating non-Kekulé molecule, the π system consists of four π electrons which can be distributed over four molecular π-type orbitals (Fig. 4). As demonstrated previously, the TMM diradical can be described in a balanced way by the SF methods;[58,65] however, the discrepancy between available experimental and theoretical multireference results was perceptible. In this section, we investigate the effect of triples on adiabatic excitation energies of four low-lying electronic states of TMM.

Two bases were used: a small 6-31G* (Ref. 66) and a larger cc-pVTZ (Ref. 50) basis sets. To compare EOM-SF-CC(2,3) results with experiment, we applied the energy separability scheme (22), where *large* and *small* correspond to the cc-pVTZ and 6-31G* bases, respectively. Equilibrium geometries and zero-point energies (ZPE) of TMM's states are from Ref. 58. Two different active spaces were employed: the minimal diradical active space ($2b_1$ and $1a_2$ orbitals) and a larger 4-π-orbital active space ($1b_1, 2b_1, 1a_2, 3b_1$).

The results for full and active space EOM-SF-CC(2,3), which are summarized in Table VI, reveal that triple excitations are very important for this system. Indeed, the inclusion of triples changes the energies of all three excited states by 0.15–0.3 eV. Note that on the EOM-SF-CCSD level, two closed-shell singlets are too high in energy, whereas the open-shell (and highly spin-contaminated) $^1B_1$ is overstabilized. This suggests that correlation of the excited states of TMM occurs by different mechanisms. Consequently, the selection of a common-to-all-states and yet compact active space is not trivial. From Table VI, the minimal two-orbital active space (similar to that employed for the CH_2 diradical) only slightly improves the EOM-SF-CCSD results. A larger four-orbital active space brings the energies of $1\ ^1A_1$ and $^1B_1$ to within 0.01 eV from full EOM-SF-CC(2,3) ones; however, the energy of $2\ ^1A_1$ is still 0.15 eV off. We noticed that in the latter state, higher in energy virtual π orbitals contribute significantly to the excitation amplitudes; therefore, a larger or different active space is required to achieve the accuracy of full EOM-CC(2,3).

TABLE VI. Total energies of the ground state (hartree) and adiabatic excitation energies (eV) of the TMM diradical calculated by different EOM-SF-CC methods in comparison to the multireference and experimental values. Equilibrium geometries and ZPEs of TMM's states as well as multireference data are from Ref. 65.

Method	$^3A_2'$	$^1B_1$	$1\ ^1A_1$	$2\ ^1A_1$
6-31 G* basis				
EOM-SF-CCSD	−155.365751	0.510	0.919	4.337
EOM-SF-CC(2,$\tilde{3}$)[a]	−155.368385	0.555	0.830	4.356
EOM-SF-CC(2,$\tilde{3}$)[b]	−155.370897	0.657	0.784	4.171
EOM-SF-CC(2,3)	−155.373271	0.653	0.774	4.028
cc-pVTZ basis				
EOM-SF-CCSD	−155.589945	0.554	0.933	3.860
EOM-SF-CC(2,3)[extrap][c]	−155.597465	0.697	0.788	3.551
MCSCF (10/10)[d]	−155.033829	0.705	0.832	
MCQDPT2 (10/10)[d]	−155.568282	0.710	0.828	
Experiment[e] $-\Delta$ ZPE[d]			0.787	

[a]EOM-SF-CC(2,$\tilde{3}$) with two-orbital active space; see text for detail.
[b]EOM-SF-CC(2,$\tilde{3}$) with four-orbital active space; see text for detail.
[c]Extrapolated results by using Eq. (22).
[d]Four frozen core and four frozen virtual orbitals.
[e]Reference 61.

The basis set effects in TMM are also state dependent. In the two lowest states, $^1B_1$ and $1\ ^1A_1$, the increase in basis set from 6-31G* to cc-pVTZ slightly raises the excitation energies, i.e., by 0.02–0.03 eV. However, in the $2\ ^1A_1$ state, there is a tremendous 0.5 eV drop in the excitation energy. The extrapolated EOM-SF-CC(2,3) results for $1\ ^1A_1$ obtained by using the energy separability scheme are in excellent agreement with the experiment. The open-shell $^1B_1$ agrees well with the MCQDPT2 data.

We conclude that for the molecule with such a nontrivial electronic structure as TMM, both dynamical and nondynamical correlations are important. Our extrapolated EOM-CC(2,3) values give an accurate estimate of the excitation energies of the considered electronic states of TMM.

D. DMX

The electronic structure of the DMX triradical was discussed in detail in Ref. 67. Molecular orbitals of DMX are given in Fig. 5. The three lowest in energy orbitals shown in this figure are doubly occupied in the lowest electronic states of DMX; the three highest in energy orbitals are unoccupied. The distribution of three electrons in three middle triradical orbitals determines the electronic state of DMX. Of these three, the lowest in energy is the a_1 orbital. This σ-type orbital is formed by the sp^2 hybridized atomic orbital on carbon and lies in the molecular plane. Two π orbitals are dominated by atomic p orbitals on the methylene carbons. According to the spin-polarization principle (and confirmed

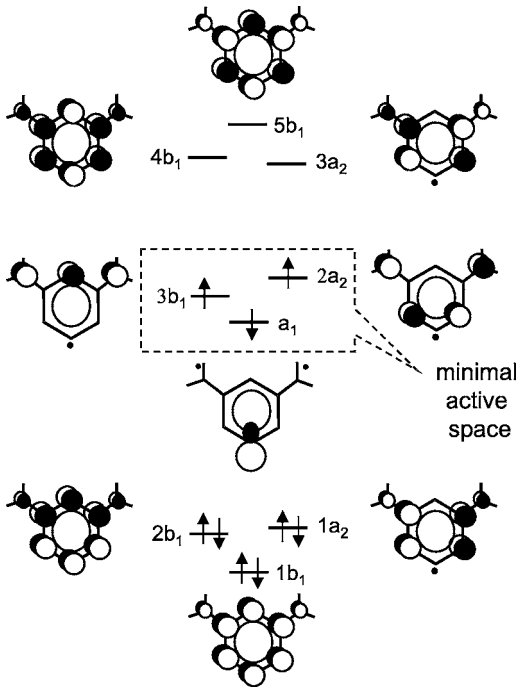

FIG. 5. Molecular orbitals of DMX. The π-system and the σ-type phenyl-like orbital are presented. Whereas the electronic state is determined by electron distribution over three triradical orbitals (minimal active space), the inclusion in active space of benzene π-orbitals is crucial for eliminating spin-contamination and producing accurate excitation energies.

by the SF calculations), the ground state of DMX is the doublet of the open-shell type, with three genuinely unpaired antiferromagnetically coupled electrons. In this state, each electron occupies its own orbital. DMX is the first example of the hydrocarbon molecule with the open-shell doublet ground state, contrary to Hund's rule and the aufbau principle.

The SF approach yields accurate energy separations between the lowest electronic states of DMX. However, the electronic states in this molecule suffer from strong spin-contamination. The spin-contamination in DMX originates from the instabilities in the σ-π-type high-spin state used as the SF reference. Similar behavior was observed in didehydrotoluens and in the $^1B_1$ (twisted) state of TMM. Here, we investigate the effect of the triple excitations on this type of spin-contamination by EOM-CC(2,$\tilde{3}$). Two active spaces were considered: the minimal triradical active space (i.e., orbitals $1a_1, 3b_1, 2a_2$ from Fig. 5) and a larger nine-orbital active space, which includes all orbitals from Fig. 5.

Two basis sets, 6-31G (Ref. 68) and 6-311G**,[49] were used in this section. To compare our results with experiment, we used the energy separability scheme of Eq. (22). The equilibrium geometry of the $^2B_2$ state is taken from Ref. 67.

The vertical energy separations between the lowest doublet and quartet states calculated at different levels of theory are given in Table VII. The spin-contamination of the reference and the excited states at the EOM-SF-CCSD level leads to the large (more than 0.3 eV!) difference between the UHF and ROHF values. Using the three-orbital active space reduces but not completely eliminates this difference. This is expected because the minimal active space does not address

TABLE VII. Total energies of the ground state (hartree) and vertical excitation energies (eV) of the DMX triradical calculated by different EOM-SF-CC methods.

Method	$^2B_2$	$^4B_2$
6-31G basis		
UHF-EOM-SF-CCSD	−307.498124	0.546
UHF-EOM-SF-CC(2,$\tilde{3}$)[a]	−307.494383	0.318
UHF-EOM-SF-CC(2,$\tilde{3}$)[b]	−307.495853	0.198
ROHF-EOM-SF-CCSD	−307.495757	0.272
ROHF-EOM-SF-CC(2,$\tilde{3}$)[a]	−307.493400	0.179
ROHF-EOM-SF-CC(2,$\tilde{3}$)[b]	−307.495619	0.158
6-311G** basis		
UHF-EOM-SF-CCSD	−308.213445	0.503
ROHF-EOM-SF-CCSD	−308.209668	0.164
UHF-EOM-SF-CC(2,$\tilde{3}$)$^{\text{extrap}}$[b,c]		0.155
ROHF-EOM-SF-CC(2,$\tilde{3}$)$^{\text{extrap}}$[b,c]		0.050
Experiment		0.04±0.17

[a]EOM-SF-CC(2,$\tilde{3}$) with three active orbitals; see text for detail.
[b]EOM-SF-CC(2,$\tilde{3}$) with nine active orbitals; see text for detail.
[c]Extrapolated results by using Eq. (22).
[d]Equilibrium geometry of the ground state of DMX and experimental data are from Ref. 67; frozen core orbitals.

the origin of the spin-contamination—mixing in to the excited state character excitations from other orbitals. Results are much more promising in the nine-orbital active space—the difference between UHF- and ROHF- based data and spin-contamination are very small (0.04 eV). We expect that the doublet-quartet separation obtained with this nine-orbital active space is very close to the full EOM-SF-CC(2,3) one.

Extrapolating the active space EOM-CC(2,3) values to the larger basis set give the results very close to ones obtained from the thermochemical experiment.[67]

IV. CONCLUSIONS

We implemented the EE and SF variants of the EOM-CC(2,3) method for computing accurate excitation energies for closed-shell systems, radicals, diradicals, and triradicals. In our implementation, both ROHF and UHF determinants can be used as a reference. Scaling of the model is N^8. The active space EOM-CC(2,3) method with semi-internal triples was also implemented; in this approach, only a small subset of triples (the number of doubles times a prefactor) is included.

The full and active space EOM-SF-CC(2,3) as well as EOM-EE-CC(2,$\tilde{3}$) are rigorously size-extensive, whereas the full EOM-EE-CC(2,3) model is only partially size-extensive.

We benchmarked the EE and SF variants of EOM-CC(2,3) on the CO^+ and CH radicals and on the CH_2 diradical. In all cases, we observed an excellent agreement between EOM-CC(2,3) and MRCI or FCI results—the errors are hundredths of eV for well-described states and up to 0.1–0.2 eV for states with significant doubly excited character. The accuracy of the active space models closely follows

that of full EOM-CC(2,3). In two larger systems, the TMM diradical and the DMX triradical, we employed the energy separability scheme to compare the EOM-CC(2,3) results with experiment. In both cases, the calculated results are in an excellent agreement with the experimental values.

The future work involves the development of transition and excited state properties and analytic energy gradients for EOM-CC(2,3).

ACKNOWLEDGMENTS

Support from the National Science Foundation CAREER Award (Grant No. CHE-0094116), the Alfred P. Sloan Foundation, and the WISE research fund (USC) is gratefully acknowledged. We thank Professor So Hirata for providing additional data on CH^+.

APPENDIX: PROGRAMMABLE EOM-CC(2,3) EQUATIONS

We solve Eq. (13) by using a generalized Davidson iterative diagonalization procedure,[69–71] which requires calculation of the products of the transformed Hamiltonian acting on trial vectors:

$$\sigma_0 = \bar{H}_{\mathrm{OS}} R_0 + \bar{H}_{\mathrm{OD}} R_0, \tag{A1}$$

$$\sigma_i^a = ([\bar{H}_{\mathrm{SS}} - E_{\mathrm{CC}}]R_1)_i^a + (\bar{H}_{\mathrm{SD}} R_2)_i^a + (\bar{H}_{\mathrm{ST}} R_3)_i^a, \tag{A2}$$

$$\sigma_{ij}^{ab} = (\bar{H}_{\mathrm{DS}} R_1)_{ij}^{ab} + ([\bar{H}_{\mathrm{DD}} - E_{\mathrm{CC}}]R_2)_{ij}^{ab} + (\bar{H}_{\mathrm{DT}} R_3)_{ij}^{ab}, \tag{A3}$$

$$\sigma_{ijk}^{abc} = (\bar{H}_{\mathrm{TO}} R_0)_{ijk}^{abc} + (\bar{H}_{\mathrm{TS}} R_1)_{ijk}^{abc} + (\bar{H}_{\mathrm{TD}} R_2)_{ijk}^{abc} + ([\bar{H}_{\mathrm{TT}} - E_{\mathrm{CC}}]R_3)_{ijk}^{abc}. \tag{A4}$$

Programmable expressions for σ including only single and double terms can be found in Ref. 24. The terms which are specific to EOM-CC(2,3) are

$$(\bar{H}_{\mathrm{ST}} R_3)_i^a = \langle \Phi_i^a | \bar{H} | R_3 \Phi_0 \rangle = 1/4 \sum_{jkbc} \langle jk || bc \rangle r_{jki}^{bca}, \tag{A5}$$

$$(\bar{H}_{\mathrm{DT}} R_3)_{ij}^{ab} = \langle \Phi_{ij}^{ab} | \bar{H} | R_3 \Phi_0 \rangle = + \sum_{kc} F_{kc} r_{kij}^{cab} + 1/2 P(ij) \sum_{klc} I_{klic}^6 r_{klj}^{cab} + 1/2 P(ab) \sum_{kcd} I_{kacd}^7 r_{kij}^{cdb}, \tag{A6}$$

TABLE VIII. H intermediates used in Eqs. (A5)–(A11).

$$H_{ia}^1 = \Sigma_{jb} r_j^b \langle ij || ab \rangle$$
$$H_{jklc}^2 = 2\Sigma_m r_m^c I_{jklm}^4 + P(jk)\Sigma_d r_j^d I_{kdlc}^1$$
$$H_{kdbc}^3 = -2\Sigma_e r_k^e I_{bced}^5 + P(bc)\Sigma_l r_l^b I_{kdlc}^1 + \Sigma_l H_{ld}^1 t_{kl}^{bc}$$
$$H_{jklc}^4 = -1/2 \Sigma_{ab} r_{jk}^{ab} I_{lcab}^7 + P(jk)\Sigma_{ai} r_{ji}^{ca} I_{lika}^6$$
$$H_{kdbc}^5 = -1/2 \Sigma_{ij} r_{ij}^{bc} I_{ijkd}^6 - P(bc)\Sigma_{ia} r_{ki}^{ba} I_{icad}^7$$
$$H_{jklc}^6 = -1/2 \Sigma_{abi} r_{jik}^{abc} \langle li || ab \rangle$$
$$H_{kdbc}^7 = -1/2 \Sigma_{aij} r_{ijk}^{bac} \langle ij || ad \rangle$$

$$([\bar{H}_{\mathrm{TT}} - E_{\mathrm{CC}}]R_3)_{ijk}^{abc} = \langle \Phi_{ijk}^{abc} | \bar{H} | R_3 \Phi_0 \rangle \tag{A7}$$

$$= P(ij|k)\left[-\sum_l F_{kl} r_{ijl}^{abc} + \sum_{lm} I_{ijlm}^4 r_{lmk}^{abc} \right] + P(ab|c)\left[\sum_d F_{cd} r_{ijk}^{abd} + \sum_{de} I_{abde}^5 r_{ijk}^{dec} \right] - P(a|bc)P(i|jk)\sum_{dl} I_{idla}^1 r_{ljk}^{dbc} + P(a|bc)P(ij|k) \times \left[-\sum_d H_{kdbc}^7 t_{ij}^{ad} + \sum_l H_{ijla}^6 t_{kl}^{bc} \right], \tag{A8}$$

$$(\bar{H}_{\mathrm{TO}} R_0)_{ijk}^{abc} = \langle \Phi_{ijk}^{abc} | \bar{H} | R_0 \Phi_0 \rangle = P(a|bc)P(ij|k) \times R_0 \left[\sum_l t_{lk}^{bc} (-I_{ijla}^2 + \sum_d t_{ij}^{ad} F_{ld}) + \sum_d t_{ij}^{ad} I_{kdbc}^3 \right], \tag{A9}$$

$$(\bar{H}_{\mathrm{TS}} R_1)_{ijk}^{abc} = \langle \Phi_{ijk}^{abc} | \bar{H} | R_1 \Phi_0 \rangle = + P(a|bc)P(ij|k) \times \left[\sum_l t_{kl}^{bc} H_{ijla}^2 + \sum_d t_{ij}^{ad} H_{kdbc}^3 \right], \tag{A10}$$

$$(\bar{H}_{\mathrm{TD}} R_2)_{ijk}^{abc} = \langle \Phi_{ijk}^{abc} | \bar{H} | R_2 \Phi_0 \rangle = P(a|bc)P(ij|k)\left[\sum_l r_{kl}^{bc} I_{ijla}^2 + \sum_d r_{ij}^{ad} I_{kdbc}^3 + \sum_l t_{kl}^{bc} H_{ijla}^4 + \sum_d t_{ij}^{ad} H_{kdbc}^5 \right]. \tag{A11}$$

I and T intermediates used in these equations are given in Table V of Ref. 24. To avoid storage of large seven-index quantities, we introduced additional intermediates that should be updated at each iteration of Davidson's diagonalization procedure. They are given in Table VIII.

[1] H. Sekino and R. J. Bartlett, Int. J. Quantum Chem., Symp. **18**, 255 (1984).
[2] H. Koch and P. Jørgensen, J. Chem. Phys. **93**, 3333 (1990).
[3] J. F. Stanton and R. J. Bartlett, J. Chem. Phys. **98**, 7029 (1993).
[4] H. Larsen, K. Hald, J. Olsen, and P. Jørgensen, J. Chem. Phys. **115**, 3015 (2001).
[5] S. Hirata, M. Nooijen, and R. J. Bartlett, Chem. Phys. Lett. **326**, 255 (2000).
[6] R. J. Bartlett, in *Theory and Applications of Computational Chemistry*,

edited by C. Dykstra, G. Frenking, K. Kim, and G. Scuseria (Elsevier, New York, 2005).
[7] H. Nakatsuji and K. Hirao, J. Chem. Phys. **68**, 2053 (1978).
[8] H. Nakatsuji, Chem. Phys. Lett. **177**, 331 (1991).
[9] J. D. Watts and R. J. Bartlett, J. Chem. Phys. **101**, 3073 (1994).
[10] J. D. Watts and R. J. Bartlett, Chem. Phys. Lett. **233**, 81 (1995).
[11] J. D. Watts and R. J. Bartlett, Chem. Phys. Lett. **258**, 581 (1996).
[12] H. Koch, O. Christiansen, P. Jørgensen, and J. Olsen, Chem. Phys. Lett. **244**, 75 (1995).
[13] O. Christiansen, H. Koch, and P. Jørgensen, J. Chem. Phys. **103**, 7429 (1995).
[14] O. Christiansen, H. Koch, and P. Jørgensen, J. Chem. Phys. **105**, 1451 (1996).
[15] S. A. Kucharsi, M. Wloch, M. Musial, and R. J. Bartlett, J. Chem. Phys. **115**, 8263 (2001).
[16] K. Kowalski and P. Piecuch, J. Chem. Phys. **113**, 8490 (2000).
[17] K. Kowalski and P. Piecuch, J. Chem. Phys. **115**, 643 (2001).
[18] M. Kállay and P. R. Surjan, J. Chem. Phys. **113**, 1359 (2000).
[19] S. Hirata, J. Chem. Phys. **121**, 51 (2004).
[20] P. G. Szalay and J. Gauss, J. Chem. Phys. **112**, 4027 (2000).
[21] C. E. Smith, R. A. King, and T. D. Crawford, J. Chem. Phys. 122 (2005).
[22] A. I. Krylov, C. D. Sherrill, and M. Head-Gordon, J. Chem. Phys. **113**, 6509 (2000).
[23] A. I. Krylov, Chem. Phys. Lett. **338**, 375 (2001).
[24] S. V. Levchenko and A. I. Krylov, J. Chem. Phys. **120**, 175 (2004).
[25] S. V. Levchenko, L. V. Slipchenko, and A. I. Krylov (unpublished).
[26] A. D. Boese, M. Oren, O. Atasoylu, J. M. L. Martin, M. Kallay, and J. Gauss, J. Chem. Phys. **120**, 4129 (2004).
[27] T. Helgaker, P. Jørgensen, and J. Olsen, *Molecular Electronic Structure Theory* (Wiley, New York 2000).
[28] D. Feller, J. Chem. Phys. **96**, 6104 (1992).
[29] K. A. Peterson, D. E. Woon, and T. H. Dunning, Jr., J. Chem. Phys. **100**, 7410 (1994).
[30] This may not be so for the high-spin (triplet or quartet) states, when the results of ROHF- and UHF-based CCSD and CCSD(T) differ considerably, as in A. M. C. Cristian, Y. Shao, and A. I. Krylov, J. Phys. Chem. A **108**, 6581 (2004).
[31] J. F. Stanton and J. Gauss, J. Chem. Phys. **101**, 8938 (1994).
[32] M. Nooijen and R. J. Bartlett, J. Chem. Phys. **102**, 3629 (1995).
[33] D. Sinha, D. Mukhopadhya, R. Chaudhuri, and D. Mukherjee, Chem. Phys. Lett. **154**, 544 (1989).
[34] A. I. Krylov, C. D. Sherrill, E. F. C. Byrd, and M. Head-Gordon, J. Chem. Phys. **109**, 10669 (1998).
[35] S. R. Gwaltney, C. D. Sherrill, M. Head-Gordon, and A. I. Krylov, J. Chem. Phys. **113**, 3548 (2000).
[36] A. I. Krylov, Chem. Phys. Lett. **350**, 522 (2001).
[37] J. S. Sears, C. D. Sherrill, and A. I. Krylov, J. Chem. Phys. **118**, 9084 (2003).
[38] J. F. Stanton, J. Chem. Phys. **101**, 8928 (1994).
[39] This follows from the fact that the similarity transformation does not not change the spectrum of the Hamiltonian, and from size consistency of the coupled-cluster wave function.
[40] H. Koch, H. J. Aa. Jensen, P. Jørgensen, and T. Helgaker, J. Chem. Phys. **93**, 3345 (1990).
[41] J. Kong, C. A. White, A. I. Krylov *et al.*, J. Comput. Chem. **21**, 1532 (2000).
[42] C. D. Sherrill and H. F. Schaefer III, Adv. Quantum Chem. **34**, 143 (1999).
[43] C. D. Sherrill, Ph. D. thesis, University of Georgia, Athens, GA, 1996.
[44] T. D. Crawford, C. D. Sherrill, E. F. Valeev *et al.*, *PSI 3.0*, PsiTech, Inc., Watkinsville, GA, 1999 (www.psicode.org)
[45] D. Maurice and M. Head-Gordon, J. Phys. Chem. **100**, 6131 (1996).
[46] Basis sets were obtained from the Extensible Computational Chemistry Environment Basis Set Database, Version, as developed and distributed by the Molecular Science Computing Facility, Environmental and Molecular Sciences Laboratory which is part of the Pacific Northwest Laboratory and funded by the U.S. Department of Energy. The Pacific Northwest Laboratory is a multiprogram laboratory operated by Battelle Memorial Institue for the U.S. Department of Energy under Contract No. DE-AC06-76RLO 1830. Contact David Feller or Karen Schuchardt for further information.
[47] A. J. Sadlej, Theor. Chim. Acta **79**, 123 (1991).
[48] G. Herzberg, *Spectra of Diatomic Molecules*, Molecular Spectra and Molecular Structure Vol. I, (Van Nostrand Reinhold, New York, 1950).
[49] R. Krishnan, J. S. Binkley, R. Seeger, and J. A. Pople, J. Chem. Phys. **72**, 650 (1980).
[50] T. H. Dunning, J. Chem. Phys. **90**, 1007 (1989).
[51] Diffuse orbitals cause problems in any active space method because, energywise, they appear in between valence occupied and virtual ones and often mix with valence orbitals. Different approaches exist to alleviate this problem, e.g., using natural orbitals instead of molecular ones.
[52] L. V. Slipchenko and A. I. Krylov, J. Chem. Phys. **118**, 9614 (2003).
[53] A. I. Krylov, J. Phys. Chem. A (submitted).
[54] Y. Yamaguchi, C. D. Sherrill, and H. F. Schaefer III, J. Phys. Chem. **100**, 7911 (1996).
[55] C. J. Cramer, F. J. Dulles, J. W. Storer, and S. E. Worthington, Chem. Phys. Lett. **218**, 387 (1994).
[56] C. W. Bauschlicher, S. R. Langhoff, and P. R. Taylor, J. Chem. Phys. **87**, 387 (1987).
[57] C. D. Sherrill, M. L. Leininger, T. J. Van Huis, and H. F. Schaefer III, J. Chem. Phys. **108**, 1040 (1998).
[58] L. V. Slipchenko and A. I. Krylov, J. Chem. Phys. **117**, 4694 (2002).
[59] P. Dowd, J. Am. Chem. Soc. **88**, 2587 (1966).
[60] R. J. Baseman, D. W. Pratt, M. Chow, and P. Dowd, J. Am. Chem. Soc. **98**, 5726 (1976).
[61] P. G. Wenthold, J. Hu, R. R. Squires, and W. C. Lineberger, J. Am. Chem. Soc. **118**, 475 (1996).
[62] C. J. Cramer and B. A. Smith, J. Phys. Chem. **100**, 9664 (1996).
[63] D. Feller, K. Tanaka, E. R. Davidson, and W. T. Borden, J. Am. Chem. Soc. **104**, 967 (1982).
[64] E. R. Davidson and W. T. Borden, J. Am. Chem. Soc. **99**, 2053 (1977).
[65] L. V. Slipchenko and A. I. Krylov, J. Chem. Phys. **118**, 6874 (2003).
[66] P. C. Hariharan and J. A. Pople, Theor. Chim. Acta **28**, 213 (1973).
[67] L. V. Slipchenko, T. E. Munsch, P. G. Wenthold, and A. I. Krylov, Angew. Chem., Int. Ed. Engl. **43**, 742 (2003).
[68] W. J. Hehre, R. Ditchfield, and J. A. Pople, J. Chem. Phys. **56**, 2257 (1972).
[69] E. R. Davidson, J. Comput. Phys. **17**, 87 (1975).
[70] K. Hirao and H. Nakatsuji, J. Comput. Phys. **45**, 246 (1982).
[71] S. Rettrup, J. Comput. Phys. **45**, 100 (1982).